Towards a surface functionalisation and grafting of a polycarbosilane onto zirconium carbide particles for the development of hybrid core-shell structures

Arish Dasan, Romain Lucas, Etienne Laborde, Cassandre Piriou, Sylvie Foucaud

▶ **To cite this version:**

Arish Dasan, Romain Lucas, Etienne Laborde, Cassandre Piriou, Sylvie Foucaud. Towards a surface functionalisation and grafting of a polycarbosilane onto zirconium carbide particles for the development of hybrid core-shell structures. Applied Surface Science, 2019, 495, pp.143409. 10.1016/j.apsusc.2019.07.151 . hal-02396888

HAL Id: hal-02396888
https://unilim.hal.science/hal-02396888v1

Submitted on 20 Jul 2022

HAL is a multi-disciplinary open access archive for the deposit and dissemination of scientific research documents, whether they are published or not. The documents may come from teaching and research institutions in France or abroad, or from public or private research centers.

L'archive ouverte pluridisciplinaire **HAL**, est destinée au dépôt et à la diffusion de documents scientifiques de niveau recherche, publiés ou non, émanant des établissements d'enseignement et de recherche français ou étrangers, des laboratoires publics ou privés.

Distributed under a Creative Commons Attribution - NonCommercial 4.0 International License

Version of Record: https://www.sciencedirect.com/science/article/pii/S0169433219321877
Manuscript_ceebd54253ea3921f2445534124c993b

Towards a surface functionalisation and grafting of a polycarbosilane onto zirconium carbide particles for the development of hybrid core-shell structures

Arish Dasan,[a] Romain Lucas*,[a] Etienne Laborde,[a] Cassandre Piriou,[a] Sylvie Foucaud[a]

[a] *Univ. Limoges, CNRS, IRCER, UMR 7315, F-87000, Limoges, France*

Corresponding author: Dr. R. Lucas, IRCER-CNRS, UMR 7315

Centre Européen de la Céramique

12 Rue Atlantis, F-87068 Limoges Cedex, France

Tel: (+)33587502350

Fax: (+)33587502304

E-mail: romain.lucas@unilim.fr

Abstract

In order to achieve future ZrC/SiC core-shell structures, hybrid ZrC-polycarbosilane materials were synthesised. To fabricate these organic coated non-oxide ceramics, the surface was first functionalised with allylchlorodimethylsilane (ACDMS) in a simple procedure. The organic covalent grafting of the carbosilane onto zirconium carbide particles was confirmed by XPS, TEM and TG-MS analyses. The effect of the temperature and of the organosilicon molecule concentration has also been investigated to check their role on the functionalisation efficiency of zirconium carbide surfaces. The modified surfaces with allyl groups were then subjected to a hydrosilylation reaction to graft a polycarbosilane. XPS, together with TG-MS and TEM images confirmed the presence of an organic coating with a thickness up to 30 nm, indicating the presence of core (ZrC)/shell (PCS) structures.

Keywords: Zirconium carbide, allychlorodimethylsilane, polycarbosilane

© 2019 published by Elsevier. This manuscript is made available under the CC BY NC user license
https://creativecommons.org/licenses/by-nc/4.0/

1. Introduction

The excellent melting point (3532–3540 °C), hardness (~25 GPa), and elastic modulus (~390 GPa) of ZrC make it an important ceramic for toughening structural materials and a promising candidate for ultra-high temperature applications [1-3]. However, a major challenge is its protection against oxidation in atmospheric conditions from a temperature of 350-400 °C. Indeed, ZrC is oxidised into ZrO_2, leading to the deterioration of the material. Therefore, it is necessary to improve the oxidation resistance of ZrC. To solve this drawback, several works focused on adding SiC into ZrC [4-6]. Thus, the incorporation of SiC could improve the oxidation resistance of ZrC by forming a protective amorphous silica layer at high temperatures [7,8]. To achieve this goal, a suitable protection strategy would be to locally coat the surface of ZrC with silicon carbide, given its good oxidation resistance at high temperatures. As the powder-mixing route is not satisfying to reach a proper core-shell structure, it was decided to use the Polymer-Derived Ceramics (PDCs) route [9-12]. Indeed, thanks to this approach, it was possible to fabricate ceramics (*e.g.* SiC) from defined polymers (*e.g.* polycarbosilane). With such a procedure, and after a suitable pyrolysis, the macromolecular network could lead to non-oxide ceramics, of which compositions depend on the polymer structure and on the elements present in the initial organometallic precursors. Nevertheless, even if this chemical pathway seems to be very attractive, the generation of core-shell systems with a strong/covalent bond linking the preceramic precursor to the inorganic material is not obvious, especially in the non-oxide ceramic field, as it is often necessary to first functionalise the surface before considering any further grafting onto the surface [13]. Interestingly, ZrC appeared to already be a core-shell structure with a layer of zirconia, which could be useful to attach small molecules with suitable functionalities to graft macromolecules in a second step [13,14]. Following this strategy, and in continuation of our efforts on this research theme [13-18], we report, in this paper, the surface modification of ZrC particles with an allylchlorosilane, followed by the grafting of polycarbosilane macromolecules, precursors of SiC ceramics. To properly monitor the steps of functionalisation and grafting leading to the hybrid objects, characterisations of the different successive materials were carried out, by using, among others, XPS, TEM, and TG-MS analyses.

2. Experimental

2.1. Materials and measurements

Allylchlorodimethylsilane (ACDMS, 97%), 1,4-diethynylbenzene (96%), diphenylsilane (97%), Platinum(0)-1,3-divinyl-1,1,3,3-tetramethyldisiloxane complex solution (Karstedt's Catalyst), diethylether (99%), di-*n*-butylether (99%) and toluene (99.8%) were obtained from Alfa Aesar. All the products were used as received. The polycarbosilane (PCS) was synthesised by the reaction of 1,4-diethynylbenzene with diphenylsilane in the presence of Pt(0) catalyst. More details were described elsewhere [18]. The ZrC used in this work was synthesized by a carbothermal reduction from a mixture of ZrO_2 (monoclinic, 99.5%, Alfa Aesar, Germany) and carbon (amorphous carbon black, 99.25%, Prolabo, France) [19]. Starting powders of zirconia (15.6 g) and carbon (4.4 g) were mixed using a low speed planetary ball mill. Then the mixture was treated at 1750 °C for 8 h in a graphite furnace (V.A.S. furnace, Suresnes, France) under flowing argon. The phase composition of the obtained powders was $ZrC_{0.96}O_{0.04}$ (04-002-5304), as detected by X-ray diffraction (Siemens D5000, Germany) using Cu Kα radiation (Figure S1, see supplementary data). To determine the grain size distribution of the zirconium carbide powder, laser granulometry analyses were performed (AccuPyc II 1340, Micro-metrics France S.A. Verneuil Halatte, France). The specific surface area (SSA) of powders was measured thanks to the gas adsorption method (ASAP 2010, Micromeritics France S.A., Verneuil Halatte, France). Samples (600 mg) were degassed at 250 °C for 12 h. Analyses were then carried out at 77 K under nitrogen (99.999%, Air liquide). The BET specific surface area was calculated from the nitrogen adsorption data in the relative pressure range from 0.05 to 0.30. Transmission electron microscopy (TEM) characterisations were carried out with a JEOL2100 microscope coupled with an Energy Dispersive X-ray Spectroscopy (EDXS) device (JEOL, Tokyo, Japan) and operating at 200 kV. The samples were prepared by crushing the powders in an agate mortar. Then they were put in suspension in a drop of water that was deposited on a copper grid covered by a holey carbon film. Heating with light made the water evaporate and the powder stick to the grid. The surface of raw and functionalised ZrC were analysed by X-ray photoelectron spectroscopy (XPS, Kratos Axis Ultra DLD spectrometer), using a monochromatic AlKα source (15 mA, 15 kV). All binding energy scales were charge referenced to the C 1s peak (285.0 eV) arising from surface contamination. The analysed area was 300 µm × 700 µm. The pass energy was 20 eV for the high-resolution spectra and 160 eV for the surveys. Simultaneous TG/DTA-MS measurements were performed with a NETZSCH STA 449 F3 apparatus coupled with a gas analysis system (OMNISTAR) in a stream of argon at a heating rate of 10 °C.min^{-1}. In order to remove the oxygen content of the system, three consecutive blank runs were carried out with a TG-sample holder, and the same Al_2O_3 crucible was used afterwards. The Zeta-potential measurements were obtained using a Zetasizer Nano ZS instrument (DLS, Malvern). The

samples were suspended in water (0.001 wt.%) and three consecutive measurements of 60 scans were recorded at 25°C for each experimental condition. An optical analyser (Turbiscan) was used to determine the stability of the functionalised zirconium carbide suspensions, grafted or not, in toluene (8.7 wt.%).

2.2. Synthesis

2.2.1. Functionalisation of ZrC surface with ACDMS

Prior to any functionalisations, the synthesised micrometric ZrC core particles were deagglomerated by using ultra-sonication in a diethylether solvent medium. In a typical procedure, 1 g of deagglomerated ZrC was dispersed in 10 mL of diethyl ether. The dispersion was treated with an excess of amount of ACDMS, 140 equiv., assuming a maximum of 10 OH per nm^2 onto the surface [13]. After 24 h of reaction at 40 °C, the mixture was separated by filtering and washing with diethylether 5 times. Finally, the resulting functionalised particles named **FZrC-40** were dried at 75 °C for 1 h. To study the effect of temperature on functionalisation, the same procedure was adopted with different temperature conditions at 60 °C, 80 °C, 100 °C and 120 °C. For these temperatures, *n*-butylether was used as a solvent instead of diethylether. Accordingly, the obtained samples were named **FZrC-T**, where T is the temperature in °C (**FZrC-60**, **FZrC-80**, **FZrC-100** and **FZrC-120**). If more equivalents of ACDMS were used, *i.e.* 280 or 420, the functionalised particles were noted **FZrCX-T***,* as the quantity of ACDMS is multiplied by 2 or 3 (*i.e.* X=2 or 3).

*2.2.2 Grafting of functionalised ZrC-ACDMS (**FZrC-40**) with a polycarbosilane (PCS)*

A 50 mL round-bottom flask was charged with 1 g of **FZrC-40** particles in 10 mL of toluene. Subsequently, 100 µl of Karstedt's catalyst were added into the suspension with magnetic stirring at room temperature for 10 minutes. Then, in 10 mL of toluene, 0.1 g of a linear polycarbosilane (PCS), of which the synthesis was described in a previous paper [18], was gradually added into the suspension. The hydrosilylation continued with constant stirring for 24 h at 75 °C. After completion, the grafted particles, named **FZrC-PCS**, were separated from the suspension by a filtration and then washed several times by toluene and finally diethylether.

3. Results and Discussion

3.1. Functionalisation of ZrC: effect of temperature/solvent and concentration

Before functionalising the non-oxide powders of ZrC, a particular attention was paid to their characterisation. The as-synthesised ZrC particles were crystalline, having a typical face-centred cubic (fcc) structure as evidenced by XRD (04-002-5304, Figure S1). Natively they display an oxide layer of roughly 5 nm depth [13]. Determined by laser granulometry, the average grain size of the starting deagglomerated ZrC powders was of 3 µm, and the surface area obtained through BET analysis was of 1.54 $m^2.g^{-1}$. This value was determined to obtain the amount of chlorosilane in excess, in order to perform a functionalisation, assuming that 10 OH per nm^2 are present on the surface. To provide suitable functional groups such as alkenes on the surface for a further grafting of a polycarbosilane by a hydrosilylation reaction, it was decided to use a nucleophilic substitution reaction with an allylchlorosilane. In this way, the hydroxyl groups of the surface [13,14], were used to functionalise the ceramic with an excess of ACDMS, at temperatures from 40 to 120 °C (Figure 1).

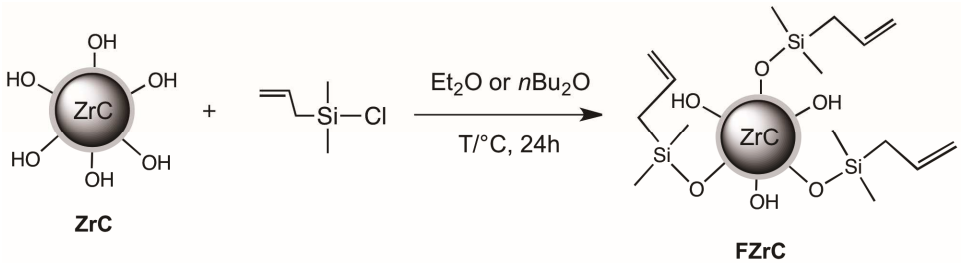

Fig. 1. Functionalisation of ZrC powders with ACDMS at different temperatures (**FZrC-T**, with T = 40, 60, 80, 100 and 120 °C).

To understand the microstructure of the bare and modified ZrC particles, and to prove the presence of the carbosilane on the surface, XPS, TG-MS and TEM coupled with EDX analyses were performed. First of all, the survey XPS spectra of every sample were recorded (Figure 2). From XPS data it was observed that the bare ZrC sample surface contained a significant amount of oxygen in addition to carbon and zirconium. This was due to the existence of an external smooth and continuous oxycarbide layer with a thickness of roughly 3 nm, as estimated thanks to higher magnification TEM images (Figure 3a).

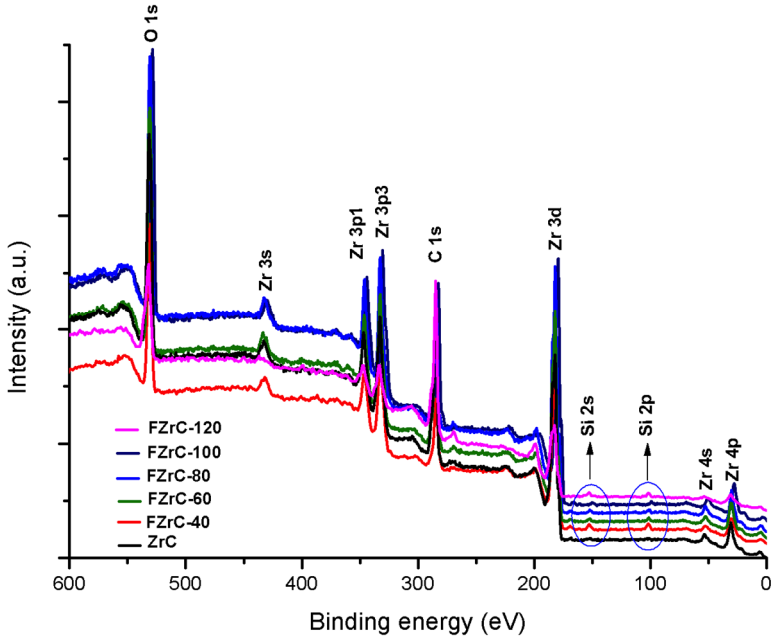

Fig. 2. The full scan XPS survey for ZrC and functionalised ZrC particles at different temperatures

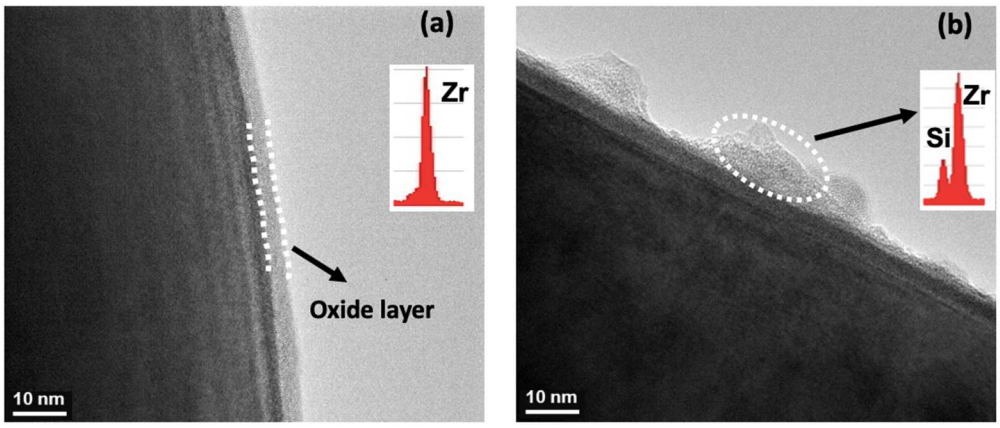

Fig. 3. Higher magnification TEM images and EDX spectrum (inset images) performed in the selected region of the oxide outer layer (a) ZrC; (b) representative spectrum of **FZrC-T**

3.1.1 Functionalisation at 40 °C: **FZrC-40**

After their surface was treated with ACDMS, silicon element signals emerged from the spectra (Figure 2). The binding energy of Si 2p of functionalised ZrC particles was located between 101 to 104 eV, which can be ascribed to the SiOZr and SiC_3O linkages respectively [13,20, 21]. The Si 2s contribution was also observed at 153 eV. Furthermore, the binding energies of C 1s, O 1s and Zr 3d were located between 282 and 288 eV, from 530 to 535 eV and from 178 to 188 eV, respectively.

They can be attributed mainly to the CC, CO, COO and CZr bonds for C 1s, OC, ZrOH, ZrOSi and ZrO bonds for O 1s, ZrO and ZrC bonds for Zr 3d (see supplementary data Figures S2-4) [22-24]. Focusing on the atomic concentrations of C, O, Zr and Si elements at the particle surface, calculated by XPS analyses (Table 1), noticeable differences were observed after functionalisation, as a significant amount of rather carbon had been added on top of the ZrC particles, *i.e.* 58.7% for **FZrC-40** in comparison with 46.9% for the bare ZrC. These results clearly demonstrated that carbon enriched ACDMS was linked onto ZrC surface *via* nucleophilic substitution reaction. Accordingly, the atomic concentration of Zr and O decreased with a loss of 9.8 and 5% respectively, being masked by the silyl functional group attached to the surface. 3.3% of silicon was also detected at the surface that was consistent with a previous study using chlorotrimethylsilane [13]. Furthermore, the obtained zeta potential value of **FZrC-40** of -26 mV was higher than that for ZrC with -5 mV. It showed more repulsive interaction between the particles than the starting powders [25], and clearly gave additional evidence of the functionalisation. To complete these results, the thermal behaviour of ZrC and **FZrC-40** was investigated (Figure 4). From the TGA analyses, a weight loss difference of less than 0.5 wt.% was observed at 1400 °C between the starting ZrC powders and **FZrC-40** (Figure 4a). Besides, the TG curve showed a slight weight loss at the beginning, and subsequently a gradual mass increase was observed from 600 °C to 1100 °C, showing a correspondence with an exothermic peak detected by DTA (Figure S5). This event was likely due to the slow kinetics of adsorption of dilute oxygen in an Ar flow. Then the weight decreased up to 1400 °C associated with the evolution of carbon dioxide as evidenced by looking at the associated mass spectra (Figure 4d). It is worth noting that even a trace amount of oxygen could react with ZrC to form zirconium oxycarbide on the surface at higher temperatures from 1000 °C to 1400 °C, which led to a weight gain on the TG curve [26, 27] On the organic side, according to the mass spectrum of **FZrC-40**, signals showed new volatile species corresponding to m/z = 15 around 380 °C (Figure 4c), not present with bare ZrC, which is unambiguously assigned to the methyl ion that was generated from the attached allyldimethylsilyl moiety. This observation could be directly correlated to the succeeded functionalisation of ZrC. Finally, a signal characteristic of hydrogen releases was also observed at temperatures of roughly 600 °C (m/z = 2, Figure 4b). This feature was evidenced with a previous theoretical study on the stability of hydrated ZrC, which showed the release of H_2 due to the dissociation of adsorbed H_2O molecules on the bare surfaces [17]. To complete these analyses, focusing on the microstructures (Figure 3), a contrast difference between the edges of starting and functionalised powder is conspicuous in the HRTEM images. Besides, the chemical compositions of the samples were analysed in the selected region by EDS under TEM, and the results clearly showed the appearance of Si peaks in the functionalised samples (Figure 3b).

Table 1. Elemental composition (atomic percentage) performed by XPS on the particle surface for ZrC, **FZrC-T**, and **FZrCX-T**

Sample	C (%)	O (%)	Zr (%)	Si (%)
ZrC	46.9	40.8	12.3	-
FZrC-40	58.7	30.7	7.2	3.3
FZrC-60	48.4	38.7	12.0	0.9
FZrC-80	50.6	37.8	10.7	0.8
FZrC-100	51.8	37.3	10.4	0.5
FZrC-120	54.6	32.2	8.8	3.7
FZrC2-40	52.8	33.4	11.3	2.6
FZrC2-120	56.6	27.6	9.1	3.7
FZrC3-40	57.8	30.3	8.5	3.3
FZrC3-120	58.4	28.8	9.4	3.4
FZrC-PCS	69.6	21.8	4.9	3.5

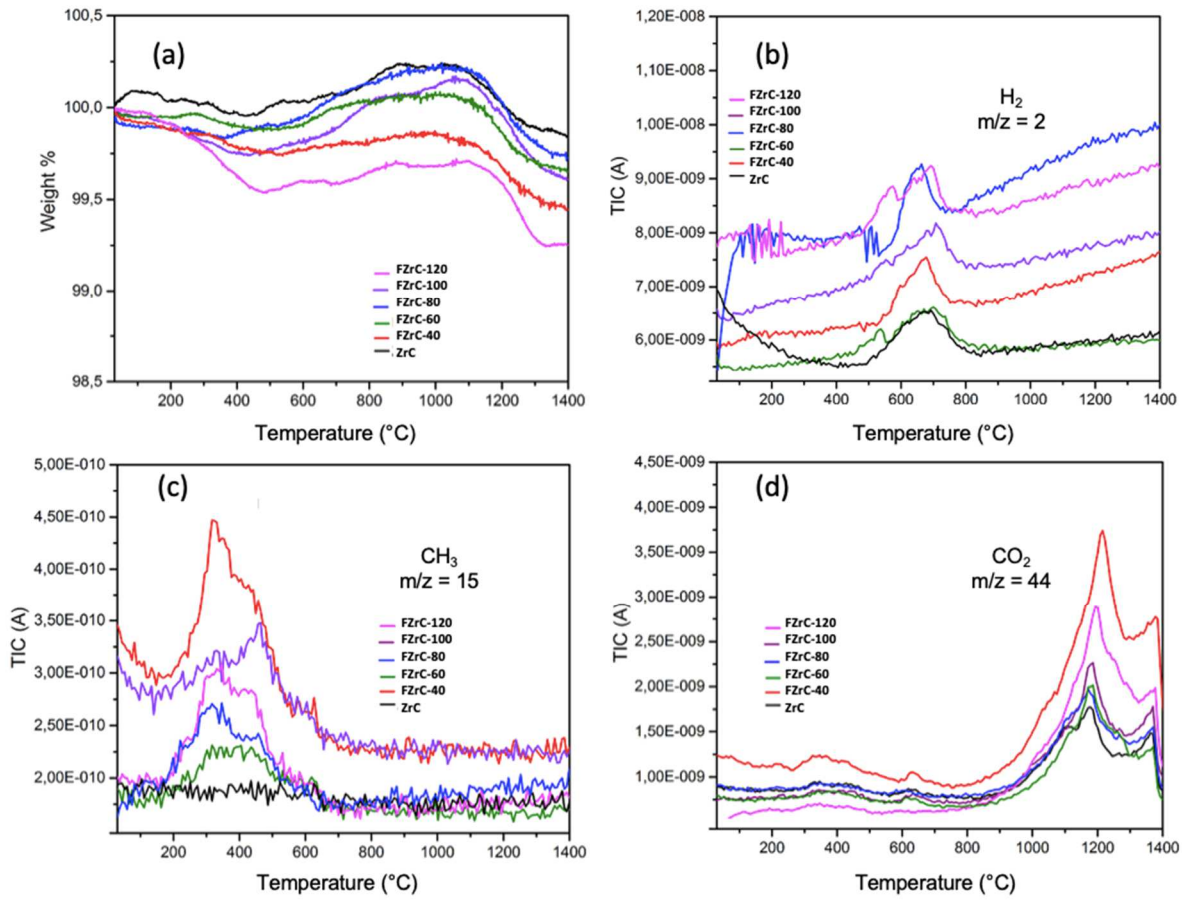

Fig. 4. Thermal decomposition pattern of ZrC and functionalised ZrC particles under argon (a) base line corrected TG-DTA curves and gas evolution curves of various of gaseous species (b) hydrogen, (c) methyl ion and d) carbon dioxide.

3.1.2 Effect of temperature/solvent and concentration

In order to assess the effect of temperature on the functionalisation, a change of solvent from diethylether to *n*-butylether was necessary. Whatever the temperature between 60°C and 120°C, silicon was detected every time on XPS spectra (Figure 2). Firstly, by comparing the elemental compositions after a functionalisation at 40 °C and 60 °C, it seemed that the resulted powders were less functionalised at a higher temperature, as only 0.9% of Si was detected (Table 1). Accordingly, the atomic concentration of Zr (12.0%) and O (38.7%) increased by 4.8 and 8% respectively, and less carbon was highlighted (only 48.4%). These results could be explained by the effect of the less polar character of *n*-butylether (μ = 1.18 D; ε = 3.1) in comparison with diethylether (μ = 1.3 D; ε = 4.33) on the nucleophilic substitution (S_N2) reaction occurring during the functionalisation, which is favoured in polar aprotic solvents. Thus, less chlorosilane would react at the surface of ZrC, leading to atomic concentrations of C, O and Zr close to the initial material. Secondly, increasing the temperature from 60 °C to 100 °C provoked a decrease in the atomic concentration of silicon at the surface from 0.9 to 0.5%. This diminution was also observed for O (from 38.7% to 37.3%) and Zr (from 12.0% to 10.4%), while the atomic concentration of carbon increased from 48.4 to 51.8%. In parallel, the carbon concentration proportion increased by 3.4%. It was required to carry out the reaction at 120 °C in order to reach 3.7% of silicon at the surface of **FZrC-120**. Looking at the TGA behaviour of **FZrC-T** with T = 40-120 °C, the five samples displayed the same trend with a total mass loss less than 1%. Focusing on the MS results, relative intensities of the methyl ion peaks were relatively higher in **FZrC-40** and **FZrC-120** compared to those of other functionalised samples (Figure 4c), which was in good agreement with the elemental analysis performed by XPS (Table 1). Furthermore, as it was previously noticed, the evolution of hydrogen (m/z = 2) around 650 °C was still observed, and CO_2 releases were detected again from 1000 °C to 1400 °C.

To try to improve the amount of carbosilane covalently linked to ZrC surface, a study was carried out on the effect of the concentration of ACDMS on the efficiency of the functionalisation. In this way, the reaction was performed with increasing, (that is doubled (280 equivalent) or tripled (420 equivalent)) the amount of ACDMS to lead to **FZrC2-T** and **FZrC3-T** samples, with T = 40 and 120 °C, as the functionalisation by ACDMS was more efficient for **FZrC-40** and **FZrC-120**. According to the XPS results (Table 1), it was found that roughly 3% of Si atoms were present on the ZrC core surface, with

no particular increase at 40 °C and 120 °C. From the TG-MS analysis, less than 1 % of weight loss was observed with the appearance of methyl ion peak (m/z = 15) around 375 °C as evidenced by the corresponding mass spectrum. TEM images also showed similar observations to those obtained in the corresponding samples functionalised with 140 equiv. From the results, however, it can be concluded that there was no clear effect on the functionalisation when increasing the concentration of ACDMS. Hence, the best compromises were to functionalise ZrC either at 40 °C or at 120 °C, with 140 equiv. of ACDMS.

*3.2. Grafting of a polycarbosilane onto **FZrC-40** surface*

FZrC-40 particles were further grafted with a polycarbosilane, a preceramic macromolecule *via* a "grafting to" approach using a hydrosilylation reaction with a platinum catalyst in toluene (Figure 5). Indeed, this preceramic precursor could be useful to generate core-shell ceramic systems, with a core of ZrC and a shell of SiC.

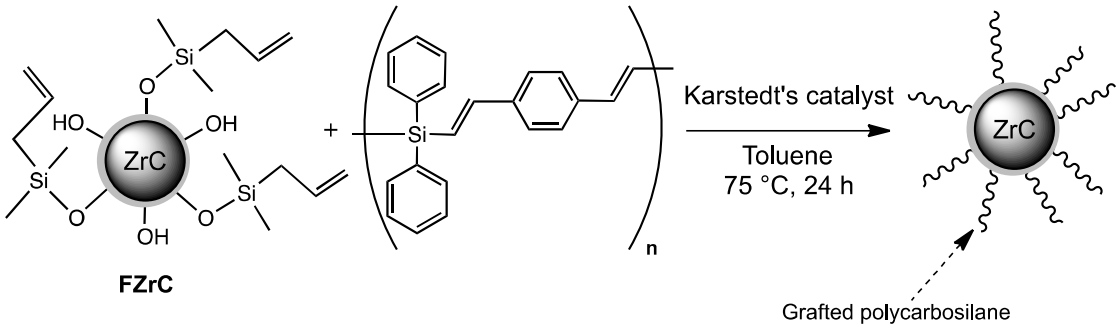

Fig. 5. Grafting reaction of a synthesised polycarbosilane onto the **FZrC-40** surface

To assess the grafting of polycarbosilane macromolecules onto the ZrC surface, several characterisation techniques were used. Firstly, a study of the stability of the suspensions was carried out with an optical analyser (Turbiscan lab, France). During the sedimentation process of **ZrC**, **FZrC-40** and **FZrC-PCS**, the transmission profiles varied with the height of the tube over time. Thus, the more the sedimentation occurred, the higher the transmission was. In this way, according to the measured transmission for an hour (Figure 6), it was possible to highlight the stability of **FZrC-PCS**, in comparison with **FZrC-40** and **ZrC**. Indeed, while **ZrC** particles seemed to settle rapidly within 8 min (Figure 6a), **FZrC-40** reached the same level of sedimentation (*i.e.* around 50%, at the top part of the tube) after 21 min (Figure 6b). This feature indicated the effect of the functionalisation on the stability of the hybrid powders. In addition, uniformly dispersed grafted **FZrC-PCS** particles were obtained, and did not transmit the light leading to a very low transmission, even after an hour (Figure 6c), proving the stability of the dispersion. Finally, to prove the necessity of using platinum to graft Si-H terminal functional groups to the alkene-functionalised surfaces, a test was performed without catalyst. This experiment gave less stable yellow coloured suspensions showing the presence of two

different populations: **FZrC-40** and the soluble PCS in toluene. It showed the importance of the presence of the platinum catalyst to perform the grafting onto the surface of functionalised ZrC.

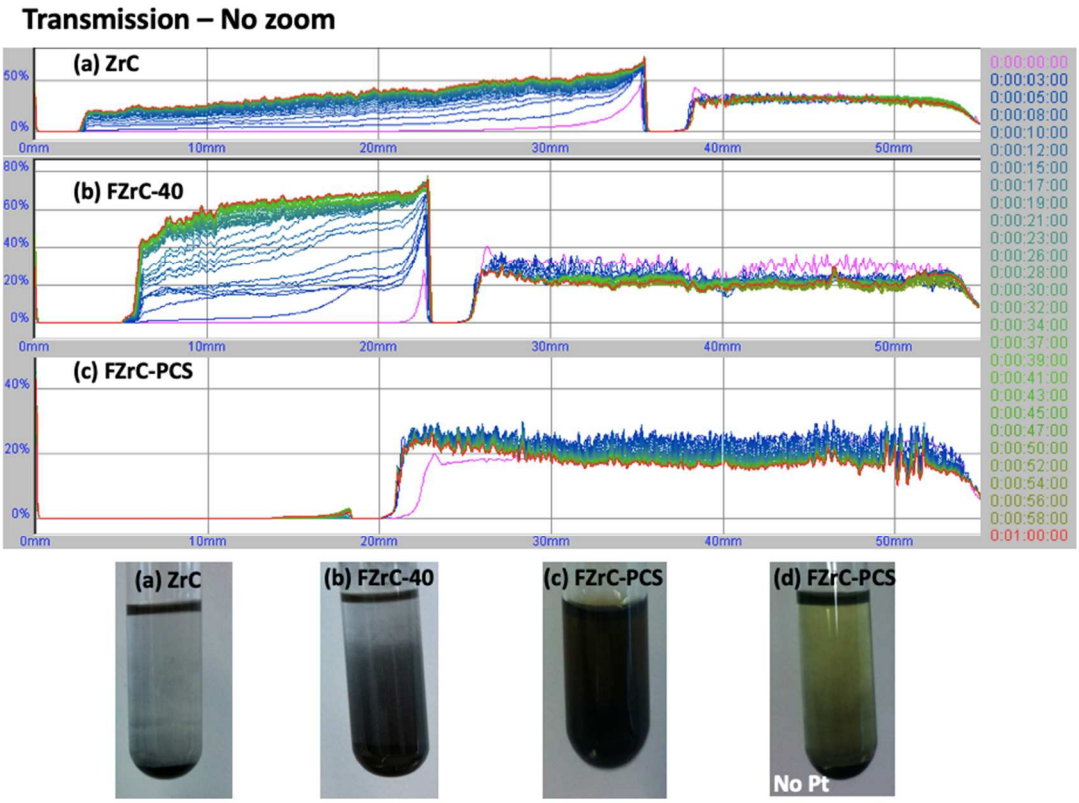

Fig. 6. Turbiscan spectra of (a) **ZrC**, (b) **FZrC-40**, (c) **FZrC-PCS** with Karsted's catalyst. The X-axis and Y-axis in the transmission diagram indicate the height of the ZrC sample tubes and the variation of transmitted light throughout the ER sample tube, respectively; and the associated dispersions in test tubes 1h after stopping stirring with (d) **FZrC-PCS without catalyst** as a comparison

To complete these results, zeta potential measurements were performed to check the impact of polycarbosilane onto the charge of ZrC surface. Thus, the obtained zeta potential value of **FZrC-PCS** was of +17.4 mV, instead of -26 mV for **FZrC-40**, clearly showing a difference on the nature of the two surfaces, and confirming the attachment of macromolecules onto **FZrC-40**. As far as we know, no previous work has been carried out on the grafting of polycarbosilane macromolecules onto "non-oxide" ceramics.

Focusing on the XPS survey, the silicon contribution was clearly observed for **FZrC-PCS** (Figure 7). The obtained binding energy of C 1s, O 1s, Zr 3d and Si 2p were relatively close to the starting FZrC-40 sample (see supplementary data Figures S6-8). The peak observed between 100.5 eV to 103.5 eV corresponded to Si 2p. According to the zoom on this signal, it was difficult to discriminate ZrO-Si bonds from Si-C linkage to the PCS, since the reported energies in PCS for Si 2p in Si-C values range

from 100.5 eV to 102.0 eV [28-30]. Nevertheless, focusing on the quantitative analysis (Table 1), the percentage of carbon element in the sample of **FZrC-PCS** was further increased to 69.6 %, while the contents of element O and Zr were changed to 21.8 % and 4.9 %, respectively in comparison with the **FZrC-40** (C, 58.7%; O, 30.7%; Zr, 7.2%). This data agreed with the presence of more organic material on ZrC particles, evidencing a hybrid core-shell structure.

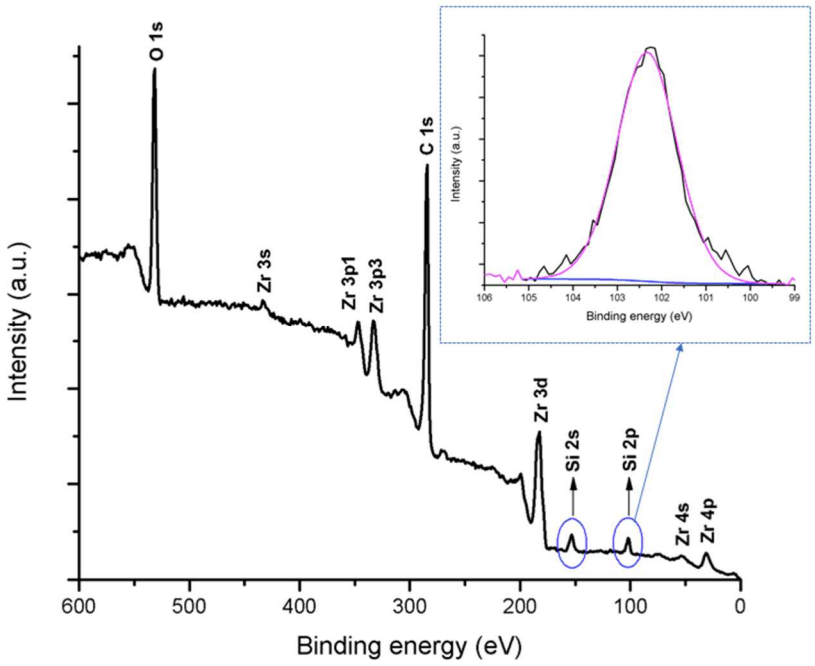

Fig. 7. XPS survey for FZrC-PCS. The insets show the high-resolution Si 2p spectrum of the corresponding samples.

The thermal behaviour of **FZrC-PCS** was also investigated (Figure 8). The TG graph displayed two continuous weight losses of roughly 10% and 6%, between 50 °C and 600 °C and from 1100 °C to 1400 °C, respectively. These releases of organic matter, more important than for **FZrC-40**, can be attributed to the decomposition of the preceramic polymer in addition to the residual solvent departure at low temperatures [18]. It is worth mentioning that even if the main mass loss up to 600°C seemed to correspond to the thermal behaviour of the preceramic polymer [18], the curve trend was the same as for **FZrC-40.** The presence of the preceramic precursor emphasised the features observed for the functionalised powders. Even if no significative mass loss was observed for the polycarbosilane above 800 °C, **FZrC-PCS** displayed a difference of 6% between 1100°C and 1400 °C. This more important mass loss than for **FZrC-40** could be explained by the possible oxidation of the free carbon generated by the polymer conversion to ceramic onto the surface of ZrC [18], leading to the detection of CO_2 (Figure 8f). Thus, the TG is not the strict addition of the behaviours of **FZrC-40**

and of the polycarbosilane (see continuous mass loss from the ambient to 600°C, while the PCS displayed a main mass loss from 400 °C to 600 °C), which means that an interaction likely existed between the two materials. Furthermore, MS measurements indicated methyl and above all phenyl fragments that were detected between 200 °C and 600 °C, in addition to hydrogen and physisorbed water molecules (Figure 8b-e) [17].

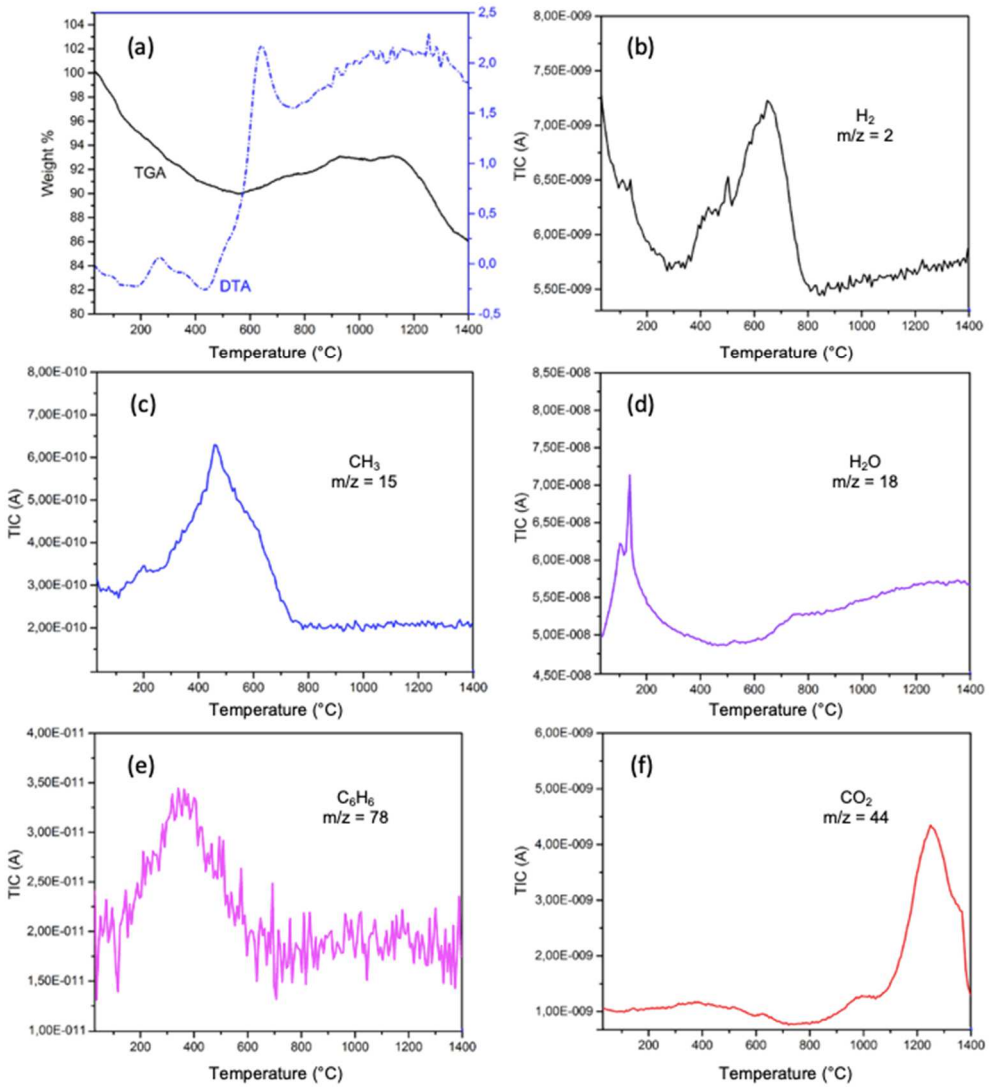

Fig. 8. Thermal decomposition pattern (under Argon) of **FZrC-PCS** (a) base line corrected TG-DTA (exo: up) curves and gas evolution curves of various species released detected with the mass spectrometer (b) H_2, (c) CH_3, d) H_2O (e) C_6H_6 and (f) CO_2.

In order to examine the attachment of PCS onto the alkene-functionalised ZrC particles at the microstructural scale, analyses were performed by TEM (Figure 9). In comparison with **FZrC40,** the results showed the presence of a thicker amorphous layer of up to roughly 30 nm onto ZrC particles

for **FZrC-PCS**. In addition, Si was detected in the shell as it is described by EDX, also proving the formation of core (ZrC)/shell (PCS) structures.

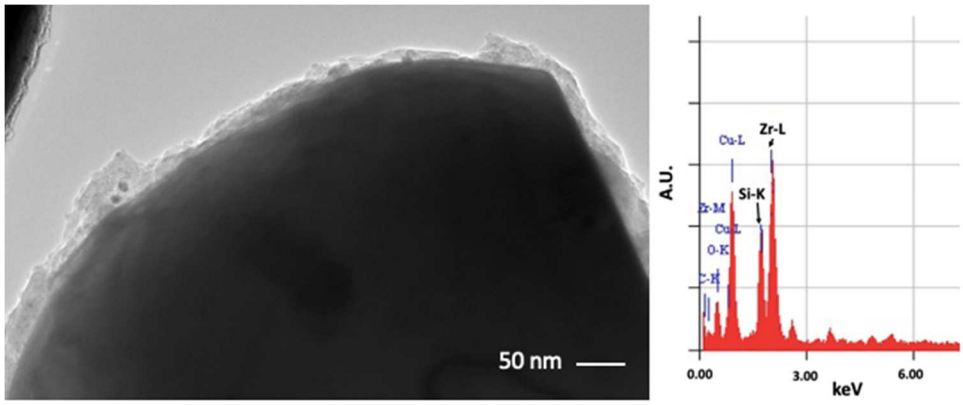

Fig. 9. TEM image of **FZrC-PCS** and EDX analysis performed in the selected region of the oxide layer

4. Conclusions

ZrC core particles were successfully functionalised with ACDMS using diethylether or *n*-butylether as a solvent and the reaction was studied with different temperature conditions and varying concentration of ACDMS. XPS, TG-MS and TEM coupled with EDX analyses indicated the attachment of ACDMS onto the ZrC surface. From the results it can also be concluded that, (i) the temperature or solvent played a vital role in the functionalisation and (ii) no clear effect was found when increasing concentration of ACDMS on functionalisation. The grafting of PCS onto the **FZrC-ACDMS** surface was further achieved via a hydrosilylation reaction. TG-MS, TEM images, the study of the stability of the suspensions and zeta potential converged towards the formation of core (ZrC)-shell (PCS) structures. Some shortcomings should also be mentioned, though, such as a lack in the real knowledge of the amount of reactive hydroxyl groups onto the surface, and then, of the generated functional groups before the grafting step. Nevertheless, quantitative analyses are currently performed to tackle this challenging obstacle, to lead to a better understanding of the reactivity of these surfaces. Eventually, this first description of a polymer grafting onto metal carbides could definitely open new horizons in the core/shell nanocomposites by employing suitable spray pyrolysis processing or other shaping.

Acknowledgements

The authors thank Jessica Roper for her help in proof reading the manuscript. They also thank the Région Limousin and for financial support. The project was also supported by the Agence Nationale

de la Recherche under Contract No.ANR-12-BS08-004-02 (CollZSiC: Elaboration de nanocomposites coeur/coquille ZrC/SiC).

References

[1] M.M.Opeka, I.G.Talmy, E.J.Wuchina, J.A.Zaykoski, S.J.Causey, J. Eur. Ceram. Soc. 19 (1999) 2405–2414.

[2] Y. Katoh, G. Vasudevamurthy, T. Nozawa, L.L. Snead, J. Nucl. Mater. 441 (2013) 718–742.

[3] R. Cano-Crespo, B.M. Moshtaghioun, D.G. García, A. D. Rodríguez, C. Retamal, M. Lagos, J. Eur. Ceram. Soc. 36 (2016) 2235–2240.

[4] M. Liang, F. Li, X. Ma, Z. Kang, X. Huang, X.G. Wang, G.J. Zhang, Ceram. Int. 42 (2016)1345–1351.

[5] C. Huang, Z. Wang, M. Wang, J. Ind Eng. Chem. 36 (2016) 80-89.

[6] Y. Li, Q. Li, Z. Wang, S. Huang, X. Cheng, Mater. Sci. Eng. A, 647 (2015), 1–6.

[7] Y. Jia, H. Li, L. Feng, J. Sun, K. Li, Q. Fu, Corros. Sci. 104 (2016) 61-70.

[8] R. Lucas, C.E. Davis, W.J. Clegg, D. Pizon, F. Babonneau, S. Foucaud, G. Antou, A. Maître, Ceram. Int. 40 (2014) 15703-15709.

[9] P. Columbo, G. Mera, R. Riedel, G.D. Sorarù, J. Am. Ceram. Soc. 93 (2010) 1805-1837.

[10] S. Yajima, K. Okamura, J. Hayashi, M. Omori, J. Am. Ceram. Soc. 59 (1976) 324-327.

[11] G. Mera, M. Gallei, S. Bernard, Nanomaterials 5 (2015) 468-540.

[12] F. Bouzat, G. Darsy, S. Foucaud, R. Lucas, Polym. Rev. 56 (2016) 187-224.

[13] R. Lucas, D. Pizon, E. Laborde, G. Trolliard, S. Foucaud, A. Maître, Appl. Surf. Sci. 287 (2013) 411–414.

[14] E. Osei, J.F. Paul, R. Lucas, S. Foucaud, S. Cristol, J. Phys. Chem. C 120 (2016) 8759-8771.

[15] D. Pizon, R. Lucas, S. Chehaidi, S. Foucaud, A. Maître, J. Eur. Ceram. Soc. 31 (2011) 2687–2690.

[16] E. Osei-Agyemang, J. F. Paul, R. Lucas, S. Foucaud, S. Cristol, J. Phys. Chem. C 118 (2014) 12952−12961.

[17] E. Osei-Agyemang, J.F. Paul, R. Lucas, S. Foucaud, S. Cristol, Phys. Chem. Chem. Phys. 17 (2015) 21401-21413.

[18] F. Bouzat, A.R. Graff, R. Lucas, S. Foucaud, J. Eur. Ceram. Soc. 36 (2016) 2913–2921.

[19] M. Gendre, A. Maître, G. Trolliard, J. Eur. Ceram. Soc. 31 (2011) 2377-2385.

[20] K.T. Jung, A.T. Bell, J. Mol. Catal. A: Chem. 163 (2000) 163 27-42.

[21] M.J. Guittet, J.P. Crocombette, M. Gautier-Soyer, Phys. Rev. B 63 (2001) 125117–125118.

[22] Y. Tang, E. Zong, H. Wan, Z. Xu, S. Zheng, D. Zhu, Microporous Mesoporous Mater. 155 (2012) 192–200.

[23] H. Zhao, B. Liu, K. Zhang, C. Tang, Nucl. Eng. Des. 251 (2012) 443-448.

[24] P.C. Wong, Y.S. Li, K.A.R. Mitchell, Surf. Rev. Lett. 2 (1995) 297-303.

[25] Liao, D L.; Wu, G S.; Liao, B Q. Zeta Potential of Shape-Controlled TiO2 Nanoparticles with Surfactants. Colloids and Surfaces A: Physicochem. Eng. Aspects 2009, 348, 270–275.

[25] S.M. El-Sheikh, Z.I. Zaki, Y.M.Z. Ahmed, J. Alloys. Compd. 613 (2014) 379–386.

[26] G.A. Rama Rao, V. Venugopal, J. Alloys. Compd. 206 (1994) 237-242.

[27] S. Shimada, T. Ishii, J. Am. Ceram. Soc., 73 (1990) 2804-2808.

[28] J. Jiao, H. Qiu, X. Li, J. Luo, Y. Wang, Key Eng. Mater. 512-515 (2012) 965-970.

[29] H. Xiaozhong, Z. Shan, C. Yong, D. Zuojuan, D. Xidong, W. Chaoying, J. Cent. South Univ. 21 (2014) 71−75.

[30] S. Chen, J. Wang, H. Wang, Mater. Des. 90 (2016) 84–90.

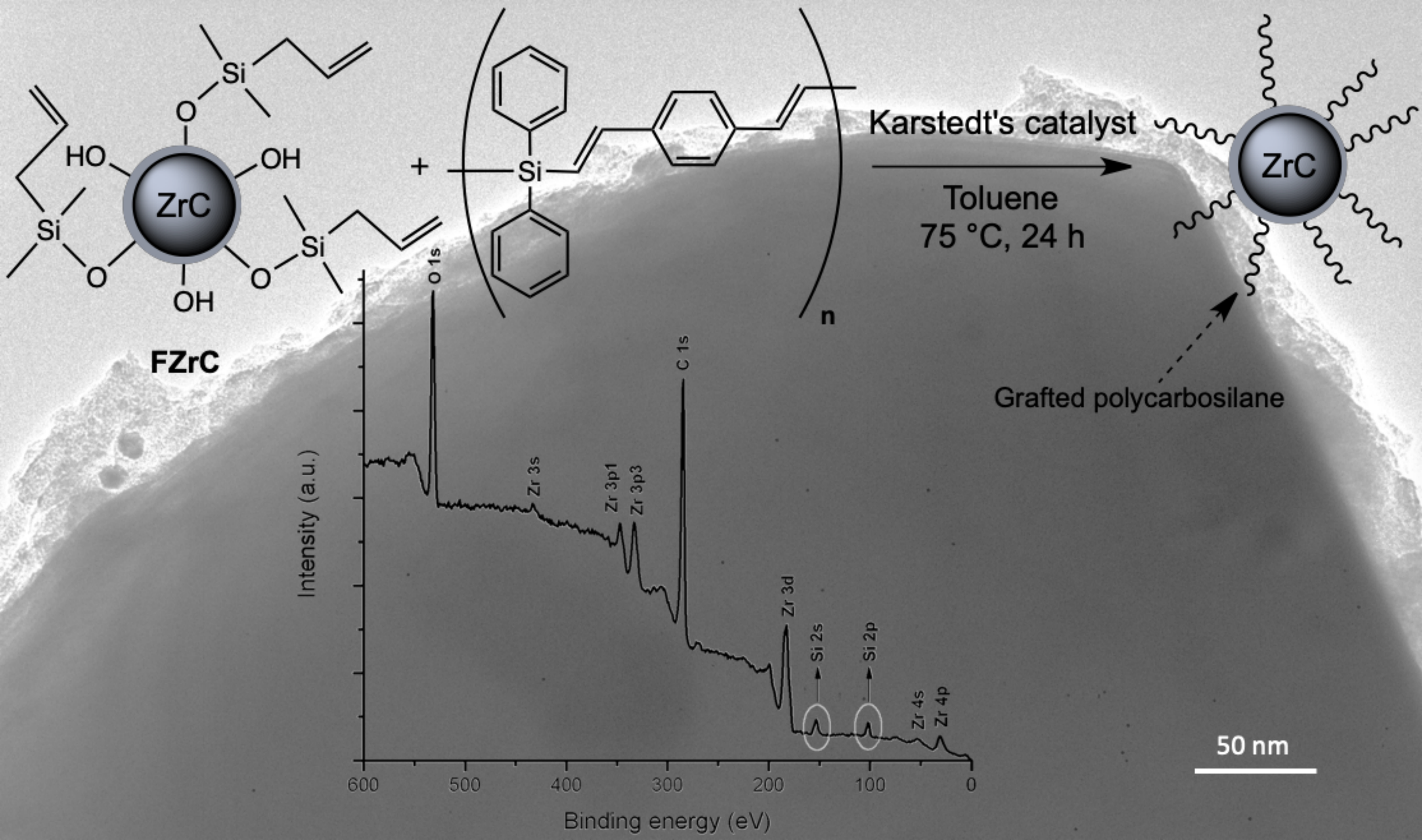
HO
OH
OH
O
Si
ZrC
FZrC
+
n
Karstedt's catalyst
Toluene
75 °C, 24 h
ZrC
Grafted polycarbosilane
50 nm
Intensity (a.u.)
Binding energy (eV)
600
500
400
300
200
100
0
O 1s
C 1s
Zr 3s
Zr 3p1
Zr 3p3
Zr 3d
Si 2s
Si 2p
Zr 4s
Zr 4p